Another mechanism for the insulator-metal transition observed in Mott insulators

Alexander G. Gavriliuk,[1,2,3] Viktor V. Struzhkin,[1] Igor S. Lyubutin,[2] Sergey G. Ovchinnikov,[4,5] Michael Y. Hu,[6] and Paul Chow[6]

[1]*Geophysical Laboratory, Carnegie Institution of Washington, 5251 Broad Branch Road NW, Washington, DC 20015, USA*
[2]*Institute of Crystallography, Russian Academy of Sciences, Leninsky Prospekt 59, Moscow 119333, Russia*
[3]*Institute for High Pressure Physics, RAS, Troitsk, Moscow Region 142190, Russia*
[4]*Institute of Physics, Siberian Division, Russian Academy of Sciences, Krasnoyarsk 660036, Russia*
[5]*Siberian Federal University, Krasnoyarsk 660041, Russia*
[6]*HPCAT and Carnegie Institution of Washington, APS, ANL, Argonne, Illinois 60439, USA*

The two widely accepted mechanisms of the insulator-metal Mott–Hubbard transitions which have been considered up until now are driven by the band-filling or bandwidth effects. We found a different mechanism of the Mott–Hubbard insulator-metal transition, which is controlled instead by the changes in the Mott–Hubbard energy U. In contrast to the changes in the bandwidth W in the "bandwidth control" scenario or to the variations of the band-filling n parameter in the "band-filling" scenario, a dramatic decrease in the Mott–Hubbard energy U plays the key role in this mechanism. We have experimentally observed this type of the insulator metal transition in the transition metal oxide $BiFeO_3$. The decrease in the Mott–Hubbard energy is caused by the high-spin–low-spin crossover in the electronic d shell of $3d$ transition metal ion Fe^{3+} with d^5 configuration under high pressure. The pressure-induced spin crossover in $BiFeO_3$ was investigated and confirmed by synchrotron x-ray diffraction, nuclear forward scattering, and x-ray emission methods. The insulator-metal transition at the same pressures was found by the optical absorption and dc resistivity measurements.

PACS number(s): 71.30.+h, 61.50.Ks, 71.27.+a, 75.30.Wx

The insulator-metal transition (IMT) in strongly correlated d-electron systems has been widely discussed since the ground-breaking work by Mott.[1] The commonly accepted mechanisms are the bandwidth controlled IMT, driven by the broadening of the d bands (e.g., by pressure), and the filling-controlled IMT, induced by the doping of charge carriers into the parent insulator compound.[2] However, up until now, the possibility to induce IMT Mott transition by the variation of the Hubbard correlation energy U has never been considered. We report here a mechanism of the insulator-metal transition, which is driven by the spin-crossover effects at high pressures in $BiFeO_3$. Our results shed light on a mechanism of IMT which is induced by the suppression of the effective Hubbard correlation energy U_{eff} at the Fe^{3+} high-spin to low-spin crossover (HS-LS) transition. These findings reveal additional complexity of electron-electron correlation effects in the d-electron system subjected to a lattice compression sufficient to overcome the Hund exchange energy; as such, the IMT mechanism is expected to be important in other spin-crossover systems. We tentatively describe this mechanism as the Hubbard energy control scenario. Notably, the HS-LS spin crossover in other Fe^{3+} oxides such as $RFeO_3$ (R is a rare earth ion)[3,4] and in $FeBO_3$ (Ref. 5) is not accompanied by the IMT, which is briefly discussed below.

Transition metal oxides constitute a very large class of materials of considerable importance for both fundamental science and practical applications. They include high-temperature superconductors, manganites with colossal magnetoresistance, multiferroics, and materials for spintronic and optoelectronic applications. Moreover, mixed iron oxides and perovskites are very important for geophysics. The properties and behavior of transition metal oxides are mainly governed by strong electron-electron correlations. It is possible to control the correlation effects by applying high pressure, and the pressure variable provides an important additional degree of freedom to study the magnetic, electronic, and optical properties of solids.

Bismuth ferrite ($BiFeO_3$) is a typical representative of transition metal oxides with strong electron correlations. It belongs to a class of multiferroic materials (ferroelectric antiferromagnet) which have both spontaneous electrical polarization and spontaneous magnetization.[6,7] Due to a record high for multiferroic antiferromagnetic Néel temperature ($T_N = 643$ K) and ferroelectric Curie temperature ($T_C = 1083$ K),[8,9] the $BiFeO_3$ crystal is most attractive for both fundamental and applied studies. It has the rhombohedrally distorted perovskite structure with space group $R3c$, and the unit cell parameters $a = 5.58$ and $c = 13.9$ A.[10,11] We have applied several high-pressure techniques[12,14] to investigate the electronic, magnetic, and structural properties of $BiFeO_3$ in highly compressed state.

The $BiFeO_3$ powder samples were prepared by the ceramic technique from stoichiometric amounts of Bi_2O_3 (99.99%) and α-Fe_2O_3 (99.99%) initial powders. Purity of the sample was controlled by x-ray diffraction. The details of the synthesis procedure could be found elsewhere.[15] To perform the resistance measurements, optical absorption, x-ray emission spectroscopy (XES),[13] nuclear forward scattering (NFS),[14] and x-ray studies at high pressures, the $BiFeO_3$ plate with the dimensions about 70×70 μm^2 was placed into a high-pressure cell with diamond anvils (DACs). The working volume of the cell was filled with the helium pressure medium for x-ray diffraction and NFS studies. Silicon oil and sodium chloride were used as pressure medium in the
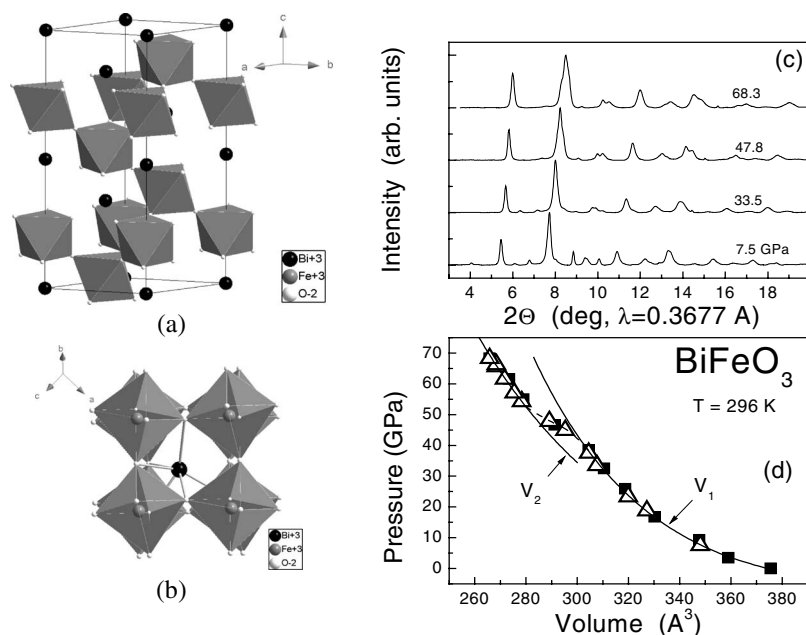
FIG. 1. (a) The unit cell structure and (b) local crystal structure of $BiFeO_3$ at normal conditions could be considered as distorted perovskite with strongly distorted FeO_6 octahedrons. (c) The evolution of x-ray patterns of $BiFeO_3$ measured in helium pressure medium does not show any change of crystal symmetry up to 70 GPa. (d) Solid lines V_1 and V_2 are the Bürch–Murnaghan approximations, indicating a structural transition between 45 and 55 GPa. This transition is caused by the spin crossover of Fe^{3+} ion. We expect a first-order-type structural transition at $T \rightarrow 0$ K due to the difference in volume of Fe^{3+} ions in HS ($S=5/2$) and LS ($S=1/2$) states. However, due to thermal (HS↔LS) fluctuations in the region of the spin crossover at $T=300$ K, the transition is broadened to about 10 GPa pressure range. Thus, we observe a broad anomaly in V-P relation indicating the transition from the high-spin to the low-spin state.

optical absorption and resistance measurements, respectively. The pressure was measured by the standard ruby fluorescence technique. Several ruby chips with dimensions of about 1 μm were placed into the cell along with the sample at different distances from the center of the working volume to evaluate the pressure gradient in the chamber. The pressure gradient was less than 0.2 GPa at all pressures for helium pressure medium and less than 2 GPa in experiments with silicon oil and sodium chloride pressure media. In the resistivity experiments, we used insulating gasket made of the mixture of cubic boron nitride with epoxy. The beryllium gasket was used in the XES measurements, and rhenium foil was used in all other types of experiments as a gasket material.

The angular-dispersive x-ray diffraction was used to investigate the crystal parameters and unit cell volume V in $BiFeO_3$ at high pressures of up to ~70 GPa at room temperature (Fig. 1). We have observed an anomaly in V-P relation in the pressure range between 40 and 50 GPa indicating a structural transition. From the Bürch–Murnaghan approximation, the bulk modulus of $BiFeO_3$ was estimated to be $B_0^{HS}=75.5 \pm 15.5$ GPa before the transition and $B_0^{LS}=292 \pm 9$ GPa after the transition [see functions V_1(P) and V_2(P) in Fig. 1(d), respectively]. We have found that during decompression measurements, the V-P relation is completely reversible.

The NFS measurements at ^{57}Fe (Fig. 2) clearly show a collapse of iron magnetic moments at pressures near 50 GPa. At room temperature, this magnetic transition is broad (from 45 to 55 GPa), and it is getting narrower with temperature decrease.

The high-pressure XES experiments [x-ray $K\beta$ emission of Fe (see Ref. [13])] have discovered dramatic changes in the spin states of iron ion Fe^{3+} in the range from 40 to 55 GPa (Fig. 2). These changes definitely indicate a spin crossover in Fe^{3+} ions from the HS state ($S=5/2$) to the LS state ($S=1/2$). The critical pressure of the spin crossover is determined by the condition $E_{HS}=E_{LS}$, where E_{HS} and E_{LS} are

energies of system in HS and LS states, respectively. We believe that the observed broad pressure range of the spin-crossover transition at room temperature [Fig. 2(b)] is due to thermal spin fluctuations between HS and LS states.[16] Such broadening was recently discovered in Gd-iron borate [$GdFe_3(BO_3)_4$] for Fe^{3+} ions[16] and in magnesiowüstite [(Mg-Fe)O] for Fe^{2+} ions.[17] We have investigated the NFS spectra at high pressures and low temperatures down to 14 K and observed a dramatic decrease in the width of the spin transition [Fig. 2(d)], in agreement with the model of thermal fluctuations between the HS and the LS states.[16] These are not spin-flip fluctuations of the spin wave type resulting from the spin vector rotations in magnetics. Instead, here we have fluctuations of the spin value between $S=5/2$ and $S=1/2$.

The effect of pressure-induced metallization was found from the optical absorption spectroscopy and the resistance measurements at high pressures both at room and low temperatures. Evolutions of optical absorption spectra and the pressure dependence of the optical gap under compression and decompression are shown in Fig. 3. At room temperature, an electronic transition is observed at pressures from 45 to 55 GPa with the optical gap decreasing to zero value [Fig. 3(c)]. This implies an insulator-metal transition in $BiFeO_3$. It is obvious that the optical gap behavior under compression follows the change of the average spin of Fe^{3+} ions during spin-crossover transition, and the gap drops to zero when the spin transition to LS state is complete.

The observed IMT was supported by the direct measurements of resistance in DAC. Pressure dependence of the resistance at room temperature is shown in Fig. 3(d). In the pressure range from 40 to 55 GPa, we observed a drop in resistance by nearly 7 orders of magnitude. The plot of the logarithm of resistance versus $-\frac{1}{4}$ power of temperature at several pressures is shown in Fig. 4(a). It is clear from Fig. 4 that at the onset of the transition, the temperature dependence of the resistance can be fitted well to the Mott formula[1] for the variable-range hopping,
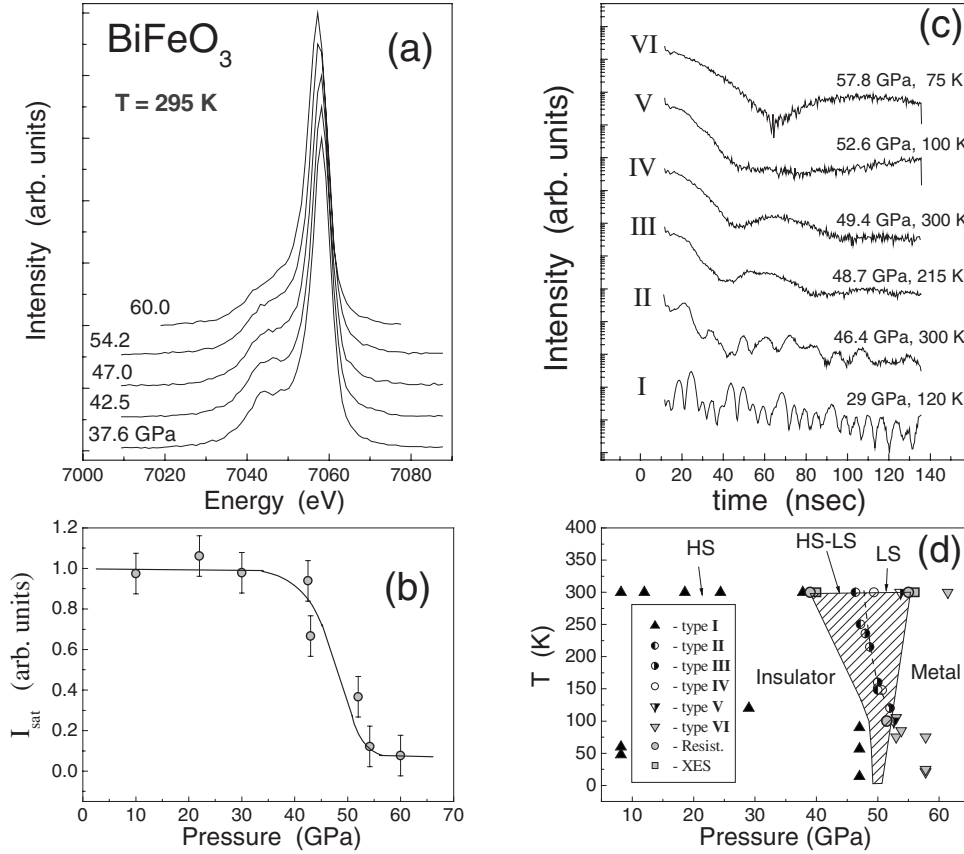
FIG. 2. [(a) and (b)] The complex scenario of electronic transition in $BiFeO_3$ at high pressure and low temperature. The evolution of XES spectra at room temperature (a) demonstrates the decrease in the satellite peak intensity in the region of 45–55 GPa (b) indicating the HS-LS spin crossover (Ref. [24]). The I_{sat} is the integrated intensity of satellite peak in arbitrary units (located on the left side from the main peak), being the measure of the high-spin value. (c) We show different types of NFS spectra observed in high-pressure–low-temperature measurements. The spectra of type I correspond to magnetic phase of Fe^{3+} ions in HS state. The spectra of type II belong to an intermediate state in the region of HS-LS spin crossover close to the HS state, type III belongs to an intermediate state in the region of HS-LS spin crossover close to the LS state, type IV is pure LS state, type V is an intermediate state at the boundary of transition from the LS (HS) state into a metal, and type VI belongs to the pure metallic phase. (d) The complex *P-T* diagram of electronic states which has the region with intermediate electronic states due to HS-LS fluctuations, the regions with pure HS (insulator) and LS (semiconductor) states, and finally, the region with LS metallic phase. At room temperature, the start and the end of the transition are bracketed by XES (gray squares) and resistance (gray circles) data. The width of the intermediate region (hatched) decreases at low temperature. The transition is narrow at 100 K [see also Fig. 4(c)]. Further experiments are required to constrain the transition width and position below 100 K.

$$R = R_0 \exp\left(\left(\frac{T_m}{T}\right)^\nu\right), \qquad (1)$$

where $\nu = \frac{1}{4}$ and T_m is the parameter of fit.

At pressures higher than 46 GPa, in the spin-crossover regime, the temperature dependence of resistance becomes more complex due to thermal spin fluctuations between the HS and the LS states. At about 55 GPa, the temperature dependence of resistance shows metallic behavior [see Fig. 4(b)] indicating the onset of the metallic state. Thus, at room temperature, the insulator-metal (IM) transition is spread over pressure range of 45–55 GPa. At lower temperature, the width of the IM transition becomes substantially reduced [Fig. 4(c)], in agreement with the thermal spin-fluctuation model.[16] In Figs. 4(d) and 4(e), we show a change of transparency of $BiFeO_3$ under pressure.

Mott[1] proposed the insulator model for transition metal oxides with partially filled *d* band. Combined with the Hubbard theory, this model predicts that the conductivity is suppressed by the strong Coulomb interaction when additional electron is added to the cation site. The effective Mott–Hubbard energy of such electron repulsion is $U_{eff}(d^5) = E(d^6) + E(d^4) - 2E(d^5)$, where $E(d^n)$ is the low term energy of the d^n configuration.[20] Below, we use a single effective Hubbard band U_{eff} (Ref. [18]) without distinguishing between the Hubbard energy U and the charge-transfer energy Δ.[19] The kinetic energy of electrons is determined by the width of the *d* band W. In this case, the fundamental gap of the insulator is equal to $(U_{eff} - W)$. The criterion of the transition from the insulating to the metallic state is $W \sim U$.[1]

Considering the pressure-induced HS-LS spin crossover in the iron borate ($FeBO_3$), Gavriliuk *et al.*[20,21] have found that the high-pressure Mott–Hubbard energy of the low-spin state U_{LS} for Fe^{3+} ion is much less than the energy of the
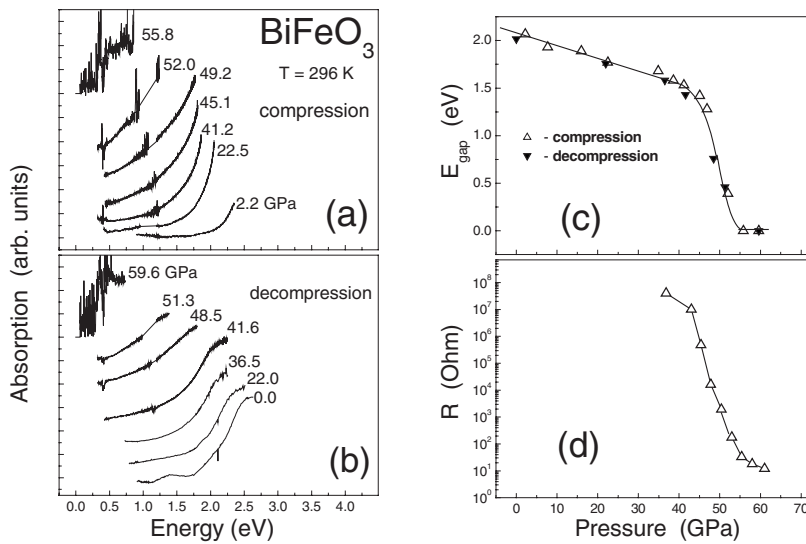
FIG. 3. The evidence for the insulator-metal transition from optical absorption and resistance measurements. The evolution of optical absorption spectra at (a) compression and (b) decompression reveals a drop of the optical gap to nearly zero in the (c) pressure range from 45 to 55 GPa. This decrease in the optical gap correlates well with the drastic drop of resistance of the sample (almost by 7 orders of magnitude) in the (d) same pressure region. The transition is continuous, and its width could be explained by the thermal HS-LS fluctuation model (Ref. 16).

low-pressure high-spin state U_{HS}, while W does not significantly change at the HS-LS transition. The difference is $U_{eff}(HS) - U_{eff}(LS) = 5J$, where J is the intraatomic Hund exchange parameter.

It appears that in the case of $BiFeO_3$, the decrease in U_{eff} at the spin crossover is sufficient to transform the crystal into the metallic state and the $W/U_{HS} < 1$ regime transforms into the $W/U_{LS} > 1$ regime,
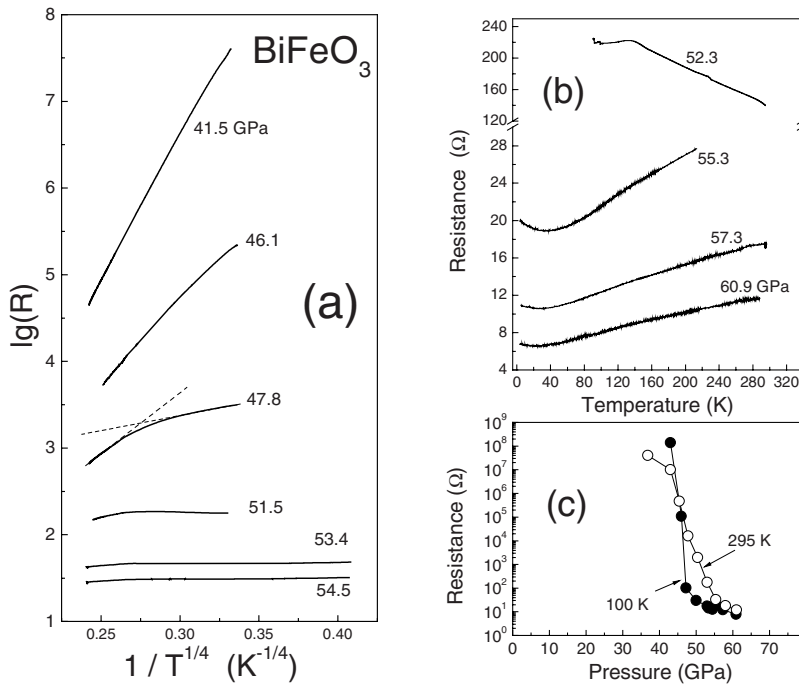
FIG. 4. (Color online) The insulator-metal transition invoked from the evolution of temperature dependence of the resistance under pressure. (a) The temperature dependence of $\log(R)$ is fitted well to the Mott dependence $\sim 1/T^{1/4}$. At pressures higher than 46 GPa, the temperature dependence becomes more complex due to the mixing of the HS and LS states in the intermediate region of the spin crossover where thermal fluctuations between the HS and LS states play an important role. (b) At about 55 GPa, the temperature dependence of resistance is changing to metallic behavior (the upturn in the resistance curves at low temperatures may be due to the nonuniform pressure distribution, when some parts of the sample remain insulating at the pressures close to IMT). The width of the insulator-metal transition at 100 K becomes substantially lower at 295 K (c) thus supporting the thermal HS-LS fluctuation model. Images of the sample at (d) 7.2 GPa and at (e) 55 GPa show the change in optical transmission of $BiFeO_3$ at the IMT. The four Pt leads are connected to the $BiFeO_3$ sample in the central hole of the cBN gasket. (d) Reddish crystal is in the center of the image; a transparent part of NaCl pressure medium is visible on the top of the sample. (e) In the image, $BiFeO_3$ sample becomes opaque because of the transition into the metallic state. At these pressures, the cBN gasket becomes nearly transparent.
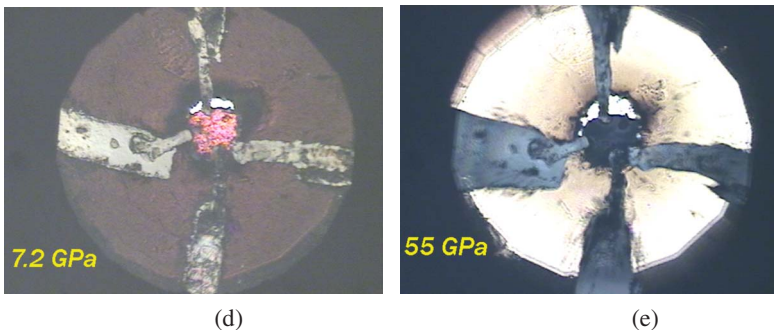
$$\frac{W}{U_{HS}} < 1 \rightarrow \frac{W}{U_{LS}} > 1. \tag{2}$$

Thus, we conclude that the electronic transition in $BiFeO_3$ is of the Mott type and it is driven by the transition of iron ions from the HS state to the LS state (spin crossover), which suppresses the Coulomb correlation energy U_{eff}, enabling the insulator-metal transition according to the Mott mechanism [Eq. (2)].

The driving mechanism for the observed transition is the reduction in the Hubbard energy U in the low-spin state. Such scenario is very different from the widely discussed band-broadening mechanism under pressure[2,22] (bandwidth control) or filling (doping) mechanism (e.g., in cuprates, manganites, etc.).[2,23]

In all experiments, we observe very similar broadening of magnetic, structural, and electronic transitions because of the unique underlying mechanism—thermal fluctuations between the HS and the LS states in the region of the spin-crossover transition. This interpretation is supported by our low-temperature data, which show the decrease in the transition width from the resistance measurements and from the low-temperature NFS experiments in helium pressure medium (Figs 2 and 4).

At the onset of the pressure-induced transition, the resistance can be fitted well to the Mott function for the variable-range hopping conductivity [Eq. (1)]. The temperature dependence of the resistance is more complex when thermal fluctuations become more important at higher pressures due to the increased concentration of the metallic phase. For example, at 47.8 GPa, there are two temperature regions, which could be fitted to the $1/T^{1/4}$ dependence with different parameters [Fig. 4(a)].

Now, we discuss why the spin crossover induced decreasing of U_{eff} results in the IMT for bismuth ferrite ($BiFeO_3$) and in the semiconductor state in iron borate ($FeBO_3$). The difference between $FeBO_3$ and $BiFeO_3$ is as follows: strong s-p bonding in BO_3 group in $FeBO_3$ results in negligible small covalency of Fe and O, thus the d-electron bandwidth is small, $W \sim 0.1$ eV.[20] The pressure-induced increase in the bandwidth in $FeBO_3$ is also small. On the contrary, in $BiFeO_3$, the covalent mixture of oxygen p and iron d electrons is not small, and the bandwidth is $W \sim 1$ eV, typical for d-metal oxides. Our calculations have shown that the bandwidth control scenario with pressure independent U_{eff} would require pressure of 250 GPa for IMT, while the spin crossover induced decrease in U_{eff} with simultaneous increase in the bandwidth results in the critical pressure of 45 GPa, which is quite close the experimental value in $BiFeO_3$.

In summary, structural, electronic, and magnetic properties have been studied at high pressures in $BiFeO_3$ crystal. The reversible insulator-metal Mott transition was observed at pressures higher than 55 GPa. The insulator-metal transition has a complex mechanism and is induced by the HS-LS crossover in the Fe^{3+} ion subsystem, which drives the effective correlation energy U_{eff} below the threshold for the IMT. The pressure-induced transition is broad and continuous at room temperature and becomes much sharper at temperature below 100 K due to suppression of thermal fluctuations between the HS state ($S=5/2$) and the LS state ($S=1/2$). The main key result of this investigation is the discovery of a mechanism of the insulator-metal transition in the Mott–Hubbard systems, which we tentatively describe as the Hubbard energy control scenario.

[1] N. F. Mott, Proc. Phys. Soc., London, Sect. A **62**, 416 (1949); Can. J. Phys. **34**, 287 (1961); *Metal-Insulator Transitions* (Taylor and Francis, London, 1990).

[2] M. Imada, A. Fujimori, and Y. Tokura, Rev. Mod. Phys. **70**, 1040 (1998).

[3] G. R. Hearne, M. P. Pasternak, R. D. Taylor, and P. Lacorre, Phys. Rev. B **51**, 11495 (1995).

[4] A. G. Gavriliuk, I. A. Troyan, R. Boehler M. I. Eremets, I. S. Lyubutin, and N. R. Serebryanaya, JETP Lett. **77**, 619 (2003).

[5] I. A. Trojan, M. I. Eremets, A. G. Gavriliuk I. S. Lyubutin, and V. A. Sarkisyan, JETP Lett. **78**, 16 (2003).

[6] A. K. Zvezdin and A. P. Pyatakov, Phys. Usp. **47**, 8 (2004).

[7] G. A. Smolenskii and I. Chupis, Sov. Phys. Usp. **25**, 475 (1982).

[8] G. A. Smolenskii, V. Yudin, E. Sher, and E. Yu. Stolypin, Sov. Phys. JETP **16**, 622 (1963).

[9] Yu. N. Venevtsev, G. Zhdanov, and S. Solovèv, Sov. Phys. Crystallogr. **4**, 538 (1960).

[10] P. Fischer, M. Polomskya, I. Sosnowska, and M. Szymanski, J. Phys. C **13**, 1931 (1980).

[11] J. D. Bucci, B. K. Robertson, and W. J. James, J. Appl. Crystallogr. **5**, 187 (1972).

[12] M. I. Eremets, *High Pressure Experimental Methods* (Oxford University Press, Oxford 1996).

[13] J. P. Rueff, C. C. Kao, V. V. Struzhkin, J. Badro, J. Shu, R. J. Hemley, and H. K. Mao, Phys. Rev. Lett. **82**, 3284 (1999).

[14] Yu. V. Shvyd'ko, Hyperfine Interact. **125**, 173 (2000).

[15] A. K. Pradhan, K. Zhang, D. Hunter, J. B. Dadson, and G. B. Loiutts, J. Appl. Phys. **97**, 093903 (2005).

[16] I. S. Lyubutin, A. G. Gavriliuk, V. V. Struzhkin, S. G. Ovchinnikov, A. M. Potseluiko, M. I. Eremets, and R. Boehler, JETP

Lett. **84**, 518 (2006).

[17] J. Lin, A. Gavriliuk, V. Struzhkin, S. Jacobsen, W. Sturhahn, M. Hu, P. Chow, and C. Yoo, Phys. Rev. B **73**, 113107 (2006).

[18] A. G. Gavriliuk, S. A. Kharlamova, I. S. Lyubutin, I. A. Troyan, S. G. Ovchinnikov, A. M. Potseluiko, M. I. Eremets, and R. Boehler, JETP Lett. **80**, 426 (2004).

[19] J. Zaanen, G. A. Sawatzky, and J. W. Allen, Phys. Rev. Lett. **55**, 418 (1985).

[20] A. G. Gavriliuk, I. A. Trojan, S. G. Ovchinnikov, I. S. Lyubutin, and V. A. Sarkisyan, JETP **99**, 566 (2004).

[21] A. G. Gavriliuk, I. A. Trojan, I. S. Lyubutin, S. G. Ovchinnikov, and V. A. Sarkissian, JETP **100**, 688 (2005).

[22] R. E. Cohen, I. I. Mazin, and D. G. Isaak, Science **275**, 654 (1997).

[23] H. Wadati, A. Chikamatsu, M. Takizawa, R. Hashimoto, H. Kumigashira, T. Yoshida, T. Mizokawa, A. Fujimori, M. Oshima, M. Lippmaa, M. Kawasaki, and H. Koinuma, Phys. Rev. B **74**, 115114 (2006).

[24] J. Badro, G. Fiquet, V. V. Struzhkin, M. Somayazulu, H. K. Mao, G. Shen, and T. LeBihan, Phys. Rev. Lett. **89**, 205504 (2002).